JGP Journal of General Physiology

ARTICLE

Constitutive activity of dopamine receptor type 1 (D1R) increases $Ca_V2.2$ currents in PFC neurons

Clara Inés McCarthy[1], Cambria Chou-Freed[1], Silvia Susana Rodríguez[1], Agustín Yaneff[2], Carlos Davio[2], and Jesica Raingo[1]

Alterations in dopamine receptor type 1 (D1R) density are associated with cognitive deficits of aging and schizophrenia. In the prefrontal cortex (PFC), D1R plays a critical role in the regulation of working memory, which is impaired in these cognitive deficit states, but the cellular events triggered by changes in D1R expression remain unknown. A previous report demonstrated that interaction between voltage-gated calcium channel type 2.2 ($Ca_V2.2$) and D1R stimulates $Ca_V2.2$ postsynaptic surface location in medial PFC pyramidal neurons. Here, we show that in addition to the occurrence of the physical receptor-channel interaction, constitutive D1R activity mediates up-regulation of functional $Ca_V2.2$ surface density. We performed patch-clamp experiments on transfected HEK293T cells and wild-type C57BL/6 mouse brain slices, as well as imaging experiments and cAMP measurements. We found that D1R coexpression led to ∼60% increase in $Ca_V2.2$ currents in HEK293T cells. This effect was occluded by preincubation with a D1/D5R inverse agonist, chlorpromazine, and by replacing D1R with a D1R mutant lacking constitutive activity. Moreover, D1R-induced increase in $Ca_V2.2$ currents required basally active Gs protein, as well as D1R-$Ca_V2.2$ interaction. In mice, intraperitoneal administration of chlorpromazine reduced native Ca_V currents' sensitivity to ω-conotoxin-GVIA and their size by ∼49% in layer V/VI pyramidal neurons from medial PFC, indicating a selective effect on $Ca_V2.2$. Additionally, we found that reducing D1/D5R constitutive activity correlates with a decrease in the agonist-induced D1/D5R inhibitory effect on native Ca_V currents. Our results could be interpreted as a stimulatory effect of D1R constitutive activity on the number of $Ca_V2.2$ channels available for dopamine-mediated modulation. Our results contribute to the understanding of the physiological role of D1R constitutive activity and may explain the noncanonical postsynaptic distribution of functional $Ca_V2.2$ in PFC neurons.

Introduction

Dopamine receptors constitute a family of G protein–coupled receptors (GPCRs) that are widely expressed in the brain and contribute to diverse neuronal functions. In particular, the D1-like receptor subfamily, which includes the dopamine receptor type 1 (D1R) and D5R, plays a key role in locomotor activity (Svensson et al., 2017) and cognitive and social behaviors (Cools, 2008; Homberg et al., 2016). The effects of D1/D5R stimulation by agonists have been thoroughly studied in behavioral tests in rodents (Zahrt et al., 1997; Stubbendorff et al., 2019) and primates (Sawaguchi and Goldman-Rakic, 1991; Arnsten et al., 2015). Moreover, there is strong evidence that different physiological and pathological states greatly correlate with changes in D1/D5R expression levels. For instance, in bird neurons, D1-like receptor mRNA increases after working memory training, while D2R mRNA remains unchanged (Herold et al., 2012). In human brains, alterations in D1/D5R receptor density and sensitivity to dopamine are associated with cognitive deficits of aging and schizophrenia (Wang et al., 1998; Thompson et al., 2014). Dopamine binding to D1/D5R receptors also changes after working memory training in humans (McNab et al., 2009). While many studies have examined these behavioral effects related to alterations in D1/D5R receptor properties, the downstream cellular events triggered by these changes remain unknown.

D1/D5R regulate working memory processes by acting mainly in the prefrontal cortex (PFC) in rodents and primates (Jones, 2002; Williams and Castner, 2006), and their expression levels in this brain area are dramatically impaired in cognitive deficit states (Goldman-Rakic et al., 2004). In particular, several studies have established a relationship between improved cognitive test performance in mice and higher levels of D1R protein specifically in the medial PFC (mPFC; Kolata et al., 2010; Wass et al., 2013, 2018). A recent report found that the origin of this D1R increase is related to the DRiP78 chaperonin (Wass et al., 2018), but their cellular targets are unknown.

[1]Electrophysiology Laboratory, Multidisciplinary Institute of Cell Biology, Universidad Nacional de La Plata, Consejo de Investigaciones Científicas y Técnicas, Comisión de Investigaciones de la Provincia de Buenos Aires, Buenos Aires, Argentina; [2]Instituto de Investigaciones Farmacológicas, Facultad de Farmacia y Bioquímica, Universidad de Buenos Aires, Buenos Aires, Argentina.

Correspondence to Jesica Raingo: jraingo@gmail.com.

Meanwhile, D1R physically interacts with voltage-gated calcium channel type 2.2 ($Ca_V2.2$) and increases channel protein density at postsynaptic sites of mPFC pyramidal neurons (Kisilevsky et al., 2008). Higher activity-mediated calcium influx could thus represent a cellular consequence of increased D1R expression levels. Here, we aimed to understand the underlying mechanisms and functional output of $Ca_V2.2$ modulation by D1R.

A relevant feature of D1R that could be involved in the increase in $Ca_V2.2$ in the plasma membrane is the receptor's constitutive activity. The importance of GPCR agonist independent activity is becoming increasingly clear (Costa and Cotecchia, 2005; Meye et al., 2014). For instance, our laboratory has demonstrated that constitutive activity of two different GPCRs has a great impact on calcium channel function (López Soto et al., 2015; Agosti et al., 2017; Mustafá et al., 2017; Martínez Damonte et al., 2018). For D1/D5R, there is an abundance of in vitro reports demonstrating a basal increase in Gs activity in several systems (Plouffe et al., 2010; Zhang et al., 2014; Zhang et al., 2015). Our studies extend the role of D1R constitutive activity in a physiologically relevant event: the stimulation of mPFC native and recombinant $Ca_V2.2$ currents by D1R expression. Moreover, we have combined the study of dopamine-mediated activity with the exploration of the role of D1R constitutive activity to modulate $Ca_V2.2$ to propose a compelling model that expands our understanding of D1R function in the brain.

Materials and methods

Animals and ethical approval

All experiments in this study received approval from the ethical committee of the Multidisciplinary Institute of Cell Biology (IMBICE), in strict accordance with the recommendations of the U.S. Guide for the Care and Use of Laboratory Animals of the National Research Council (reference number from the Ethical Committee of IMBICE; #12-03-19). All possible actions to minimize suffering were taken. Experiments were conducted on C57BL/6 WT mice of both sexes. Mice were bred and housed at the IMBICE animal facility with a 12-h light/dark cycle, controlled room temperature (22°C ± 2°C), and ad libitum access to food and water.

Animal treatment and PFC slice preparations

A total of 18 mice were used in this study (vehicle, n = 11; chlorpromazine-treated, n = 7). 4–6-wk-old WT mice were treated with vehicle (saline solution NaCl 0.9%) or chlorpromazine (1 mg/kg) through two intraperitoneal (IP) injections (0.1 ml/10 g) 24 h and 1 h before sacrifice. Mice were anaesthetized with isoflurane (2%) and immediately decapitated. Brains were quickly removed and immersed in ice-cold 95% O_2 and 5% CO_2-equilibrated cutting solution containing (in mM) 110 choline chloride, 25 glucose, 25 $NaHCO_3$, 7 $MgCl_2$, 11.6 ascorbic acid, 3.1 sodium pyruvate, 2.5 KCl, 1.25 NaH_2PO_4, and 0.5 $CaCl_2$, pH 7.4, with CsOH. Coronal brain slices including the mPFC (~300 µM, 1.5–2.5 mm anterior to bregma) were obtained using a vibratory tissue slicer (PELCO easiSlicer; #11000; Ted Pella Inc.) and then transferred to an incubation chamber filled with 95% O_2, 5% CO_2–equilibrated artificial cerebrospinal fluid (aCSF) containing (in mM) 124 NaCl, 26.2 $NaHCO_3$, 11 glucose, 2.5 KCl, 2.5 $CaCl_2$, 1.3 $MgCl_2$, and 1 NaH_2PO_4, pH 7.4, with HCl. Slices were maintained at 37°C for 15 min and left to recover at room temperature (~24°C) for 30 min before recordings.

Cell culture and transient transfections

HEK293T cells were grown in Dulbecco's modified Eagle's medium (DMEM; #D5030, Gibco; Thermo-Fisher) with 10% FBS (Internegocios A.S.) and subcultured when 80% confluence was reached. For patch-clamp experiments, HEK293T cells were cotransfected with plasmids containing human D1R (*DRD1*; GenBank accession no. NM000794), kindly provided by Dr. M. Tiberi (University of Ottawa, Ottawa, ON, Canada), the human D1RS199A (Al-Fulaij et al., 2008), and voltage-gated calcium channel subunit $Ca_V2.2$ (*Cacna1b*; GenBank accession no. AF055477) with auxiliary subunits $Ca_V\beta_3$ (*Cacnb3*; GenBank accession no. M88751) and $Ca_V\alpha_2\delta_1$ (*Cacna2d1*; GenBank accession no. AF286488). Cells were cotransfected with a fixed amount of $Ca_V2.2$ and the following increasing amounts of D1R cDNA: 11, 17, and 23 ng per well (equivalent to D1R:$Ca_V2.2$ molar ratios of 0.05, 0.075, and 0.1, respectively). For some experiments, cells were additionally transfected with plasmids containing cDNA encoding a peptide corresponding to the D1R loop 1, D1R loop 2, or C terminus of $Ca_V2.2$ (0.2 µg cDNA transfected per well for saturating expression). For live imaging experiments, YFP-tagged versions of D1R and D1RS199A mutant were used. All transient transfections were conducted using Lipofectamine 2000 (#11668019, Invitrogen; Thermo-Fisher) and, whenever necessary, an enhanced GFP (eGFP) containing plasmid to identify transfected cells and the empty plasmid pcDNA3.1 (+) to complete the total cDNA amount in the transfection mix were added. Transfected HEK293T cells were kept in culture for 24 h to allow expression, then dispersed with 0.25 mg/ml trypsin, rinsed twice, and kept in DMEM at room temperature during patch-clamp experiments.

For FRET time course of cAMP intracellular level experiments, stable HEK293T-expressing pcDNA3.1/Zeo(1)-mTurquoise2-EPAC-cp173Venus-Venus (Epac-S H187) (HEKT Epac-S H187) cells were obtained by transfection of HEK293T using the K2 Transfection System (Biontex). 24 h after transfection, cells were seeded in the presence of 25 µg/ml Zeocin (InvivoGen) for 2 wk, and clonal selection was performed in 96-well plates for 2 wk. Clones were tested for Epac-S H187 by fluorescence spectra (450–650 nm) measurements in a FlexStation 3 Multi-Mode Microplate Reader (Molecular Devices) with excitation at 430 nm. The HEKT Epac-S H187 clone with higher fluorescence emission was chosen for further experiments. The stable clone was grown in DMEM medium supplemented with 10% FBS, 50 µg/ml gentamicin, and 12.5 µg/ml Zeocin. For transient transfections, HEK293T and HEKT Epac-S H187 cells were grown to 80–90% confluency. cDNA constructs were transfected into cells using the K2 Transfection System. The transfection protocol was optimized as recommended by the supplier. Assays were always performed 48 h after transfection. The expression of the constructs was confirmed by immunoblotting using specific antibodies. The mTurquoise2-EPAC-cp173Venus-Venus

(Epac-S H187) construct was provided by Dr. KeesJalink (Cell Biophysics and Imaging Group, Netherlands Cancer Institute, Amsterdam, Netherlands; Klarenbeek et al., 2011).

Cloning

Plasmids containing cDNA encoding the D1R loop 1 (including amino acids 52–57) or D1R loop 2 (including amino acids 118–138) peptides were kindly provided by Dr. G. Zamponi (University of Calgary, Calgary, AB, Canada), originally included in pGEX-5.1 bacterial expression vectors. To express D1R loop 1 and D1R loop 2 in a mammalian system, the sequences for D1R loop 1 and D1R loop 2 were cloned by blunt ligation into a pcDNA6 vector backbone containing IRES-eGFP. The previously characterized D1RS199A mutant (Al-Fulaij et al., 2008) was generated through directed mutagenesis using the commercial plasmid containing the human D1R (*#DRD0100000*; cDNA Resource Center, University of Missouri). To generate YFP-tagged versions of D1R and D1RS199A mutant, the sequences without stop codon were amplified by PCR with a sense oligonucleotide containing an EcoRI site and an antisense oligonucleotide containing a BamHI site. The PCR fragment was digested with EcoRI and BamHI and inserted into EcoRI and BamHI sites of PRK6-YFP vector. The proximal portion of the $Ca_V2.2$ C terminus was amplified by PCR with a sense oligonucleotide primer containing BamHI, an ATG codon 5207–5222, and nucleotides 5207–5222 of $Ca_V2.2$ and antisense oligonucleotide primer containing a PsyI site followed by a stop codon and nucleotides 6037–6023 of $Ca_V2.2$. The sequence for the proximal portion of the $Ca_V2.2$ C terminus was subcloned into pcDNA6 vector backbone containing IRES-eGFP. All the final constructs were Sanger-sequenced by Macrogen.

Drugs

The commercial antipsychotic drug chlorpromazine (chlorpromazine HCl, 25 mg/ml injectable blister, CAS #50–53-3; Laboratorios Duncan S.A.) was donated by Dr. Martinez Mónaco and Dr. Pinedo (Italian Hospital of La Plata, Buenos Aires, Argentina) and used for IP injections in mice and 20-h preincubations of transfected HEK293T cells. Chlorpromazine stock solution was stored at room temperature, protected from light, and dissolved in saline solution 0.9% NaCl <24 h before IP injections. For patch-clamp recordings from mouse mPFC slices, the sodium channel blocker tetrodotoxin (1 µM; CAS #4368–28-9, #T8024; Sigma-Aldrich), the $Ca_V2.2$ blocker ω-conotoxin-GVIA (1 µM; CAS #106375–28-4, #C-300; Alomone Labs), dopamine hydrochloride (CAS #62–31-7, #H8502; Sigma-Aldrich), (±)-1-phenyl-2,3,4,5-tetrahydro-(1H)-3-benzazepine-7,8-diol hydrochloride (SKF-38393; 10 µM; CAS #62–717-42-4, #D047; Sigma-Aldrich), and (−)-quinpirole hydrochloride (40 µM; CAS #85798–08-9, #Q102; Sigma-Aldrich) were used. Dopamine was also used in patch-clamp experiments in HEK293T cells. Cholera toxin (ChTx; 500 ng/ml; CAS #9012–63-9, #C8052; Sigma-Aldrich) was used for 20-h preincubations in transfected HEK293T cells in order to block Gs protein activity.

Electrophysiology

Calcium channel currents were recorded with either an EPC7 (HEKA Electronik) or an Axopatch 200 (Molecular Devices) amplifier. Data were sampled at 20 kHz and filtered at 10 kHz (−3 dB) using either PatchMaster (HEKA Electronik) or pCLAMP8.2 (Molecular Devices) software. Access resistance and input resistance were monitored by a step of −10 mV. Recordings in which the access resistance increased by >20% were discarded. Leak current was subtracted online using a P/−4 protocol, and recordings with leak currents over 150 pA at holding potential were discarded.

Native calcium currents of mPFC pyramidal neurons

Acute coronal mouse brain slices were transferred to the recording chamber and visualized with an upright Zeiss Examiner.A1 microscope (#491404–0001-000), a digital camera (Rolera Bolt Scientific CMOS; QImaging), and Micro-Manager 1.4 open source microscopy software (Vale Lab, University of California, San Francisco). Layer V/VI pyramidal neurons of the mPFC were identified by localization and morphology (Wang et al., 2006). Whole-cell patch-clamp recordings in voltage-clamp mode were conducted at room temperature (~24°C) in the previously described aCSF (2.5 mM Ca^{2+}) under a continuous flow rate of 2.5 ml/min. Recording electrodes with resistances between 3 and 6 MΩ were used and filled with internal solution containing (in mM) 115 Cs-methanesulfonate, 20 tetraethylammonium chloride, 10 CsCl, 5 NaCl, 10 HEPES, 10 EGTA, 4 Mg-ATP, and 0.3 Na-GTP, pH 7.4, with CsOH.

For native calcium current recordings, tetrodotoxin (1 µM) was added to normal aCSF (2.5 mM Ca^{2+}) to block native voltage-gated sodium channels. Neurons were held at resting potential (−80 mV), and native calcium currents were evoked applying square pulses from −80 to 0 mV (60-ms duration), with a subsequent step at −60 mV (30-ms duration) before returning to resting potential. Additionally, the specific $Ca_V2.2$ blocker ω-conotoxin-GVIA (1 µM) was added to analyze $Ca_V2.2$ contributions to total native calcium currents. Whenever indicated, 10 µM dopamine, 10 µM SKF38393, 40 µM quinpirole, or 10 µM chlorpromazine was acutely applied to the bath solution.

Calcium currents in transiently transfected HEK293T cells

Whole-cell patch-clamp recordings were performed in transfected HEK293T cells in voltage-clamp mode. Recording electrodes with resistances between 2 and 5 MΩ were used and filled with internal solution containing (in mM) 134 CsCl, 10 HEPES, 10 EGTA, 4 MgATP, and 1 EDTA, pH 7.4, with CsOH. All recordings were conducted at room temperature (~24°C) with an external solution containing (in mM) 140 choline chloride, 10 HEPES, 1 $MgCl_2.6H_2O$, and 2 $CaCl_2.H_2O$, pH 7.4, with CsOH. To evoke ionic $Ca_V2.2$-mediated currents in HEK293T cells, square pulses from −100 to 10 mV (30-ms duration) followed by a step at −60 mV (10-ms duration) were used. Cells were held at −100 mV as resting potential. ON gating current recordings were performed with square pulses from −100 mV to the reversal potential. The reversal potential was determined by calculating the 0 current point in a current-voltage curve built with square voltage pulses (5-ms duration) from −100 to 55–70 mV every 0.5 mV. The datasets for each experimental condition were obtained from at least three independent experiments.

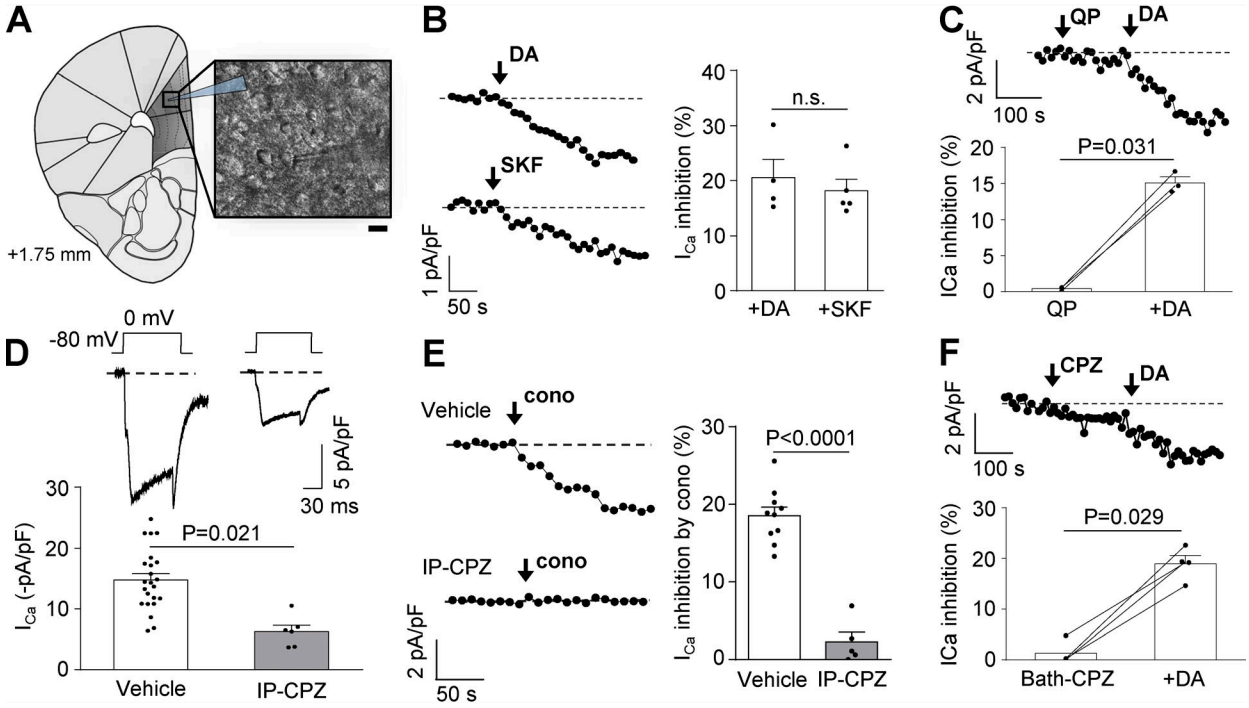

Figure 1. **Ca_V currents from mPFC neurons are sensitive to D1/D5R constitutive and agonist-evoked activity. (A)** Schematic coronal slice of a mouse brain containing the mPFC (1.75 mm anterior to bregma), showing the location of the patch pipette in layer V of the mPFC (dark gray area). Inset shows an infrared differential interference contrast image illustrating a recorded layer V/VI pyramidal neuron. Scale bar represents 10 µm. **(B)** Representative time courses and averaged values of percentage of Ca_V current (I_{Ca}) inhibition from mPFC neurons by dopamine (+DA; 10 µM; *n* = 4, three animals) and SKF38393 (+SKF; 10 µM; *n* = 5, three animals). **(C)** Representative time course of I_{Ca} and averaged values for the percentage of I_{Ca} inhibition from mPFC neurons by subsequent application of quinpirole (QP; 40 µM) and dopamine (+DA; 10 µM; *n* = 3, two animals). **(D)** Representative traces and averaged normalized I_{Ca} registered in mPFC of mice treated IP with vehicle (*n* = 23, eight animals) or chlorpromazine (CPZ; 1 mg/kg; *n* = 6, four animals). **(E)** Representative time courses of I_{Ca} and averaged percentage of inhibition of I_{Ca} by acute application of ω-conotoxin GVIA (cono; 1 µM) from mPFC neurons of mice treated IP with vehicle (*n* = 10, six animals) or CPZ (1 mg/kg; *n* = 5, four animals). **(F)** Representative time course of I_{Ca} and averaged values for the percentage of inhibition of I_{Ca} from mPFC neurons by subsequent application of 10 µM CPZ and 10 µM dopamine (+DA; *n* = 4, three animals). Student's unpaired (B, D, and E) and paired (C and F) *t* test. n.s., nonstatistically significant. Data were expressed as mean ± SEM, and dots represent individual data points.

Imaging

24 h after transfection with D1R-YFP (11 or 23 ng of cDNA per well) or D1RS199A-YFP (23 ng per well), cells were washed twice with 1× PBS, and 0.5 ml of 1 µg/ml membrane marker solution (CellMask orange plasma membrane stain; Molecular Probes) was added for 1 min, then cells were washed a third time with PBS. Finally, the PBS was removed, and a clean coverslip was placed over the cell layer. Fluorescence photomicrographs were obtained using an optical epifluorescence microscope (Eclipse Nikon 50i) at 60× magnification (0.80-mm numerical aperture), equipped with B2A and G2A filters and a camera (DS-Ri1; Nikon Corp.). Image acquisition was performed using the Nis-Elements F 3.2 software (Nikon Corp.). FIJI ImageJ open source software was used to analyze the photomicrographs and to calculate total green fluorescence intensity, which was normalized by cell area. The datasets for each experimental condition were obtained from at least three independent experiments.

FRET time course of intracellular cAMP (i-cAMP)

FRET time course of cAMP intracellular levels was measured as previously described (Carozzo et al., 2019). Briefly, HEKT Epac-S H187 cells transfected with D1R, D1R plus D1R loop 2, or empty pcDNA3.1 (+) plasmid was seeded in 96-well plates at a density of 10^5 cells per well. Before each experiment was started, cells were washed with 0.9% NaCl twice, and 100 µl of FluoroBrite DMEM (Thermo-Fisher) was added to each well before placing the plate in a FlexStation 3 at 37°C. To determine i-cAMP response, the baseline fluorescence signal detected at 475 nm (donor) and 530 nm (FRET) emission with excitation at 430 nm was measured. Using the on-board pipettor, 50 µl of dopamine or chlorpromazine 3 µM stock solution (to reach a final concentration of 1 µM in the well) or FluoroBrite DMEM was added after 40 s, and then the signals were monitored every 20 s for a total of 600 s. FRET and donor intensities were measured for each time point. FRET/donor ratio was calculated and normalized to basal levels before stimulation (R/R_0) for each time point. An area under the curve value of 9-min R/R_0 i-cAMP response was calculated for each replicate.

Basal i-cAMP measurement

cAMP levels measured in HEK293T cells transfected with D1R, D1R plus D1R loop 2, or empty pcDNA3.1 (+) were performed as in Agosti et al. (2017). Briefly, 24 h after transfections, the supernatants were removed, and 0.8 ml of ethanol was added to each well. Ethanol was dried out, and residues were resuspended with 50 mM Tris-HCl, pH 7.4, with 0.1% BSA. cAMP

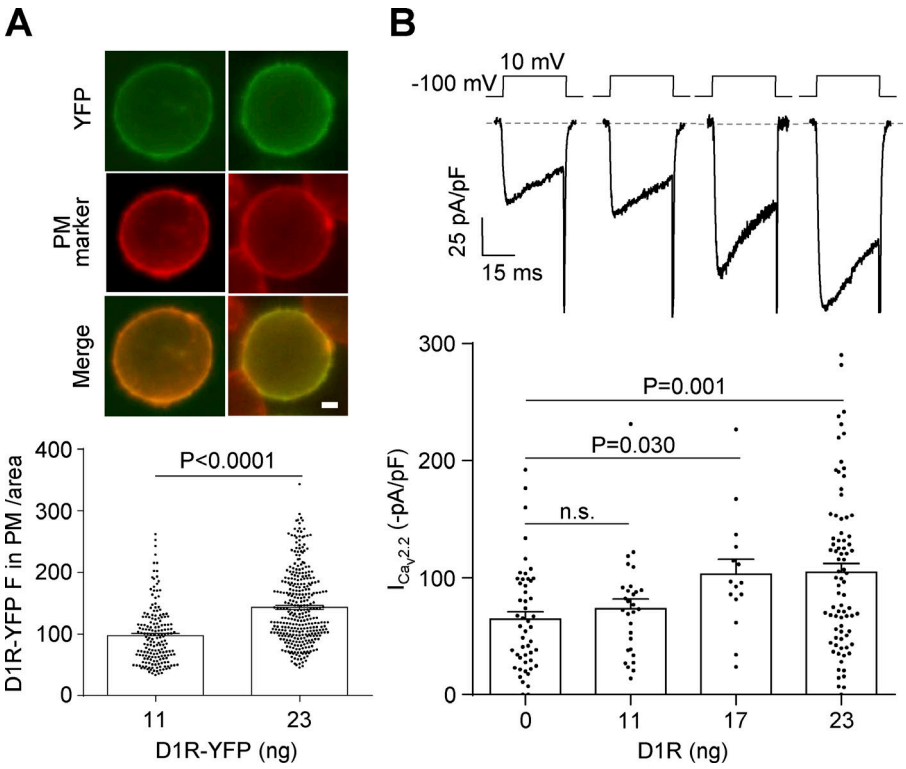

Figure 2. **The sole expression of D1R increases $Ca_V2.2$ currents in transfected HEK293T cells. (A)** Photomicrographs and average YFP fluorescence (D1R-YFP F) in the plasma membrane (PM) normalized by cell area in HEK293T cells co-transfected with $Ca_V2.2$, $Ca_V\alpha_2\delta_1$, $Ca_V\beta_3$, and two different amounts of D1R-YFP (11 and 23 ng cDNA per well, equal to 0.05 and 0.1 D1R:$Ca_V2.2$ molar ratios, respectively). Green and red signals originate from the YFP tag on D1R and the PM marker CellMask (PM marker), respectively. Scale bar represents 1 µm. **(B)** Representative traces and averaged $Ca_V2.2$ currents ($I_{Cav2.2}$) from HEK293T cells co-transfected with $Ca_V2.2$, $Ca_V\alpha_2\delta_1$, $Ca_V\beta_3$, and increasing amounts of D1R (0–23 ng cDNA per well). Student's unpaired *t* test (A) and Kruskal-Wallis test with Dunn's post-test versus 0 ng D1R (B). n.s., nonstatistically significant. Data were expressed as mean ± SEM, and dots represent individual data points.

content was determined by a competitive radio-binding assay for PKA using [3H]-cAMP as previously described (Davio et al., 1995). The standard curve was performed using eight cAMP concentrations ranging from 0.1 to 90 pmol. Duplicate samples in at least three independent experiments were analyzed.

Statistics

Data were analyzed and visualized using OriginPro 8 (Origin-Lab Corp.) and Prism 6 (GraphPad Software Inc.) software. We used the Kolmogorov–Smirnov test for conformity to a normal distribution, and variance homogeneity was examined using Bartlett's (normally distributed data) and Brown–Forsythe's (nonnormally distributed data) tests. P values were calculated from Student's paired and unpaired *t* test and multiple comparisons one-way ANOVA with Dunn's or Tukey's post hoc tests (normally distributed data) or from the Mann–Whitney test or Kruskal–Wallis test with Dunn's post hoc test (nonnormally distributed data). Concentration-response curves for dopamine were fitted with Hill equations. Lineal regressions for area under the gating current recorded for each cell (Q_{ON}) versus peak tail current were compared by extra sum-of-squares F test. The specific statistical test used and sample size for each dataset are indicated in the figure legends, including P values. Data were expressed as mean ± SEM, and dots represent individual data points.

Results

Chlorpromazine, a D1/D5R inverse agonist, reduces total Ca_V currents in mPFC neurons

First, we tested the hypothesis that D1R constitutive activity plays a role in controlling $Ca_V2.2$ current density in mPFC neurons. We obtained acute coronal brain slices and recorded native Ca_V currents from layer V/VI pyramidal neurons of the mPFC (Fig. 1 A). We first ran control experiments to assay the capability of D1/D5R to modulate Ca_V currents by comparing the effect of acute application of dopamine (10 µM) and SKF38293 (SKF; 10 µM), a specific D1/D5R agonist. We found that these two agonists equally reduced the currents (Fig. 1 B). Moreover, dopamine in the presence of 40 µM quinpirole, a D2R agonist, had a similar effect (Fig. 1 C). Thus, we conclude that D1/D5R are the main dopamine receptor subtypes modulating Ca_V currents in mPFC neurons. To study D1/D5R constitutive activity, we took advantage of the fact that several antipsychotic drugs, including chlorpromazine, have been shown to act not only as D2R antagonists but also as inverse agonists of D1/D5R (Cai et al., 1999). Therefore, we evaluated if pretreatment with chlorpromazine is capable of reducing $Ca_V2.2$ currents in mPFC pyramidal neurons. We performed two consecutive IP injections in mice with 1 mg/kg chlorpromazine or vehicle 24 h and 1 h before the experiment and found that native Ca_V currents from chlorpromazine-treated mice were significantly smaller than currents from vehicle-treated mice (~51% of the total current in control; Fig. 1 D). Next, we assessed the contribution of $Ca_V2.2$ to the total calcium current affected by chlorpromazine and found that the sensitivity of Ca_V currents to 1 µM ω-conotoxin GVIA was dramatically reduced from ~18% to ~2% in chlorpromazine-treated mice, suggesting that inhibiting D1/D5R constitutive activity reduces $Ca_V2.2$ currents (Fig. 1 E). Finally, we explored the effect of acute subsequent bath application of chlorpromazine and dopamine on Ca_V currents from vehicle-treated mice. We found no effect of chlorpromazine, indicating the requirement of an extended period of time for this effect, and 20% of Ca_V current inhibition by dopamine, similar to the values obtained in panels B

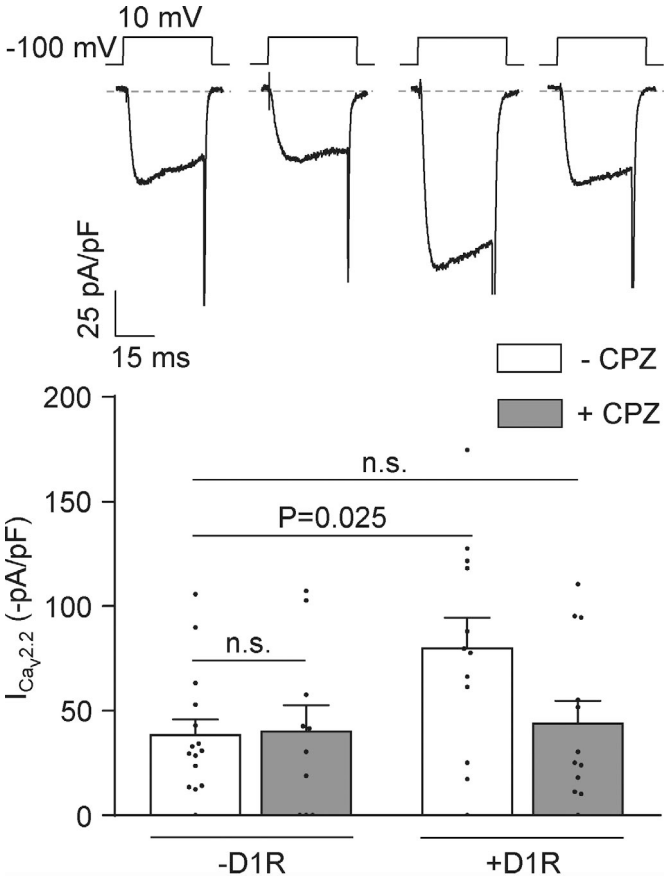

Figure 3. **Chlorpromazine occludes D1R-induced increase in $Ca_V2.2$ currents in transfected HEK293T cells.** Representative traces and averaged $Ca_V2.2$ currents ($I_{Cav2.2}$) from HEK293T cells cotransfected with $Ca_V2.2$, $Ca_V\alpha_2\delta_1$, $Ca_V\beta_3$, and either D1R (+D1R −CPZ; n = 12) or empty plasmid (−D1R −CPZ; n = 15), preincubated (+D1R +CPZ; n = 12) or not (−D1R +CPZ; n = 10) with chlorpromazine (CPZ; 1 µM). One-way ANOVA with Dunn's post-test versus −D1R −CPZ. n.s., nonstatistically significant. Data were expressed as mean ± SEM, and dots represent individual data points.

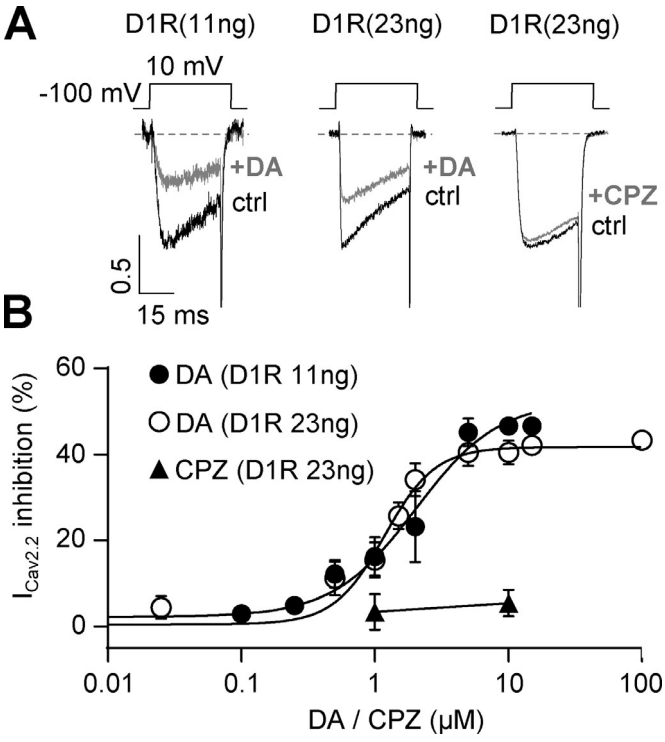

Figure 4. **Acute application of dopamine but not chlorpromazine inhibits $Ca_V2.2$ currents in transfected HEK293T cells. (A)** Representative traces of $Ca_V2.2$ currents from HEK293T cells transfected with $Ca_V2.2$, $Ca_V\alpha_2\delta_1$, $Ca_V\beta_3$, and D1R (11 or 23 ng cDNA) before and after acute application of dopamine (+DA; 10 µM) or chlorpromazine (+CPZ; 10 µM). **(B)** Concentration-response curve for dopamine (+DA) and chlorpromazine (+CPZ; n = 3, 1 µM and n = 4, 10 µM) effect on $Ca_V2.2$ currents ($I_{Cav2.2}$). Data on dopamine effect were fitted with Hill equations for each D1R cDNA amount used (EC_{50} = 2.023 µM for 11 ng, total n = 42, r^2 = 0.77 and EC_{50} = 1.180 µM for 23 ng of D1R, total n = 61, r^2= 0.86). EC_{50}, half-maximal effective concentration. Data were expressed as mean ± SEM.

and C (Fig. 1 F). In summary, our data suggest that pyramidal neurons from mPFC display lower $Ca_V2.2$ currents when D1/D5R constitutive activity is reduced.

D1R coexpression increases $Ca_V2.2$ currents in transfected HEK293T cells

To study the effect of D1R coexpression on isolated $Ca_V2.2$ currents, we used a heterologous expression system that we previously proved effective for studying the agonist-independent activity of other GPCRs (López Soto et al., 2015; Agosti et al., 2017). We cotransfected HEK293T cells with two different amounts of YFP-tagged D1R (D1R-YFP) cDNA and a fixed amount of $Ca_V2.2$ and its auxiliary subunits. We first confirmed that increasing the amount of transfected D1R-YFP cDNA significantly increased the total fluorescence intensity (Fig. 2 A). Next, we evaluated the size of $Ca_V2.2$ currents in cells transfected with a range of D1R cDNA and found that increasing the amount of D1R cDNA dramatically increased $Ca_V2.2$ currents (Fig. 2 B). Thus, we found that higher D1R expression levels led to increased $Ca_V2.2$ basal currents.

Agonist-independent activity of D1R increases $Ca_V2.2$ currents

Assuming that each D1R molecule displays a fixed level of constitutive activity, our data presented in Fig. 2 allow us to propose that D1R agonist-independent activity contributes to positively modulate $Ca_V2.2$ currents. We therefore tested if preincubation with the D1/D5R inverse agonist chlorpromazine prevents this stimulatory effect. Indeed, we found that 10 µM chlorpromazine preincubation occludes $Ca_V2.2$ current increase by D1R coexpression, while having no effect on control currents (Fig. 3). On the other hand, the drug failed to directly affect $Ca_V2.2$ currents, as we found no effect of acute application of chlorpromazine at the concentration used for preincubation in cells expressing only $Ca_V2.2$ (percent $I_{CaV2.2}$ inhibition by 10 µM chlorpromazine = 2.6 ± 1.0%; n = 5; nonstatistically significant from zero, one-sample t test). We ran additional control experiments to confirm that D1R is functional in our system and the lack of effect from acute application of chlorpromazine on D1R- and $Ca_V2.2$-expressing cells. We found that dopamine application inhibits $Ca_V2.2$ currents in a concentration-dependent manner. Moreover, increasing the amount of D1R cDNA in the transfection mix had no effect on dopamine-mediated inhibition. Finally, we failed to observe an effect

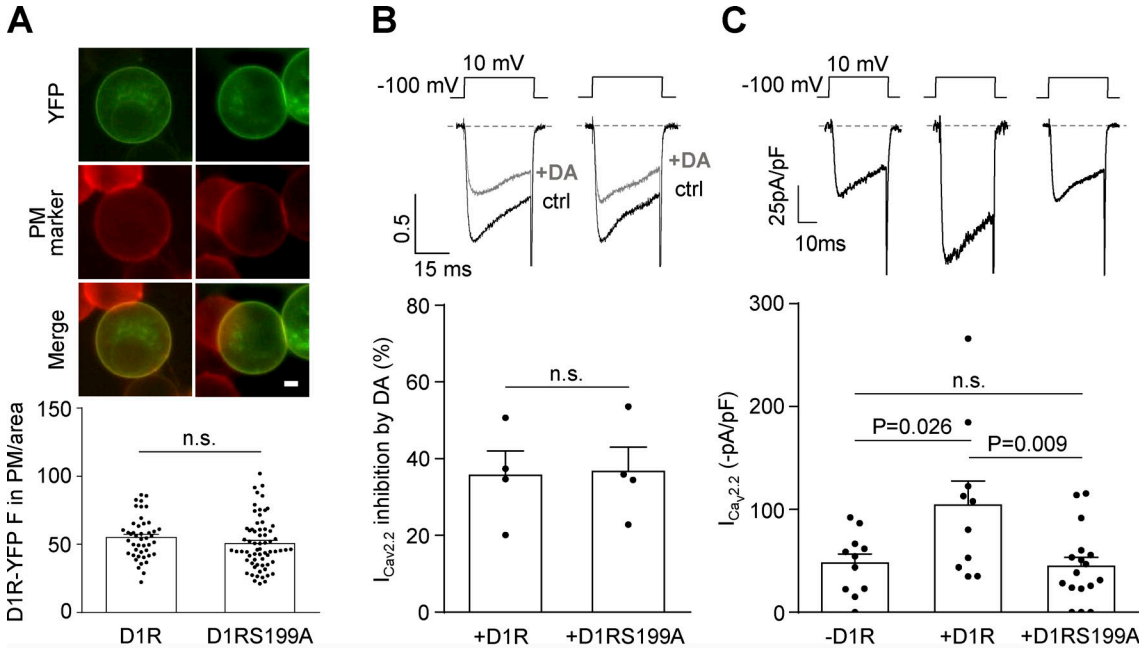

Figure 5. **D1RS199A mutant with impaired constitutive activity fails to increase $Ca_V2.2$ currents. (A)** Photomicrographs and average YFP fluorescence (D1R-YFP F) signal in the plasma membrane normalized by cell area (D1R-YFP in PM/area) in HEK293T cells transfected with D1R-YFP or D1RS199A-YFP. Green and red signals originate from the YFP tag on D1R or D1RS199A and the plasma membrane marker CellMask (PM marker), respectively. Scale bar represents 1 µm. **(B)** Representative traces and averaged percentage of $Ca_V2.2$ current ($I_{Cav2.2}$) inhibition by dopamine (+DA; 10 µM) in HEK293T cells coexpressing $Ca_V2.2$, $Ca_V\alpha_2\delta_1$, $Ca_V\beta_3$, and D1R (+D1R; $n = 4$) or D1RS199A (+D1RS199A; $n = 4$). **(C)** Representative traces and averaged $I_{Cav2.2}$ from HEK293T cells cotransfected with $Ca_V2.2$, $Ca_V\alpha_2\delta_1$, $Ca_V\beta_3$, and either empty plasmid (−D1R; $n = 11$), D1R (+D1R; $n = 10$), or D1RS199A (+D1RS199A; $n = 17$). Student's unpaired t test (A and B) and one-way ANOVA with Tukey's post-test (C). n.s., nonstatistically significant. Data were expressed as mean ± SEM, and dots represent individual data points.

of acute application of chlorpromazine in this experimental setting (Fig. 4), similar to our result on native currents (Fig. 1 F). Together, our data from Figs. 2, 3, and 4 indicate that D1R constitutive activity is required for $Ca_V2.2$ current increase and also recapitulate our observations using chlorpromazine on native Ca_V currents from mouse mPFC pyramidal neurons.

Previous studies reporting D1R agonist–independent activity have used D1R mutants with diminished constitutive activity as genetic tools (Zhang et al., 2014). We chose a single mutant, D1RS199A, that displays a very low level of constitutive activity but maintains the same expression levels and sensitivity to dopamine as WT D1R (Al-Fulaij et al., 2008). We first checked that the expression level of YFP-tagged versions of WT and mutant D1R were the same (Fig. 5 A). We also compared the inhibitory effect of acute application of dopamine on $Ca_V2.2$ currents and found no differences between D1RS199A and WT D1R in our experimental conditions (Fig. 5 B). Next, we compared basal $Ca_V2.2$ currents and found that D1RS199A failed to increase basal $Ca_V2.2$ currents (Fig. 5 C). Thus, our data suggest that only constitutively active D1R is capable of increasing $Ca_V2.2$ current.

Channel-receptor physical interaction is required for D1R-induced increase of $Ca_V2.2$ currents

We next evaluated if the effect of D1R on $Ca_V2.2$ involves physical channel-receptor interaction. This hypothesis arises from published work proposing that D1R loop 2 and the proximal region of $Ca_V2.2$ C terminus interact, stimulating the traffic of $Ca_V2.2$ proteins to the cell membrane (Kisilevsky et al., 2008). This report shows that a peptide with the sequence of D1R loop 2 competes with D1R for interaction with the channel, while other peptides, including one with the D1R loop 1 sequence, do not. Based on these observations, we assayed the effect of expressing either D1R loop 2 or 1 on the $Ca_V2.2$ current increase caused by D1R coexpression. We found that D1R loop 2 indeed occludes the current increase, while D1R loop 1 has no effect (Figs. 6, A and B). We also assayed the effect of coexpressing a 277–amino acid peptide corresponding to the $Ca_V2.2$ C terminus and found that this maneuver also prevents the current increase by D1R coexpression (Fig. 6 C). Finally, we verified that the acute inhibitory effect of dopamine in these experimental conditions was intact (Fig. 6 D). These results indicate that the $Ca_V2.2$ current increase driven by D1R requires that constitutively active D1R physically interact with $Ca_V2.2$.

D1R constitutive activity increases gating $Ca_V2.2$ currents

To explore if the increased $Ca_V2.2$ current that we observed in transfected HEK293T cells is related to a higher channel density at the plasma membrane, we recorded gating currents, a metric of the number of functional channels expressed at the cell surface. We recorded ON gating currents at the reversal potential (around +60 mV) from a resting potential of −100 mV. We calculated the charge movement as Q_{ON}, normalized by the cell capacitance (Castiglioni et al., 2006). We observed that D1R coexpression increases the Q_{ON}, and, consistent with our previous results, D1R loop 2 coexpression and D1R replacement by D1RS199A occluded this effect (Fig. 7 A). To demonstrate that the

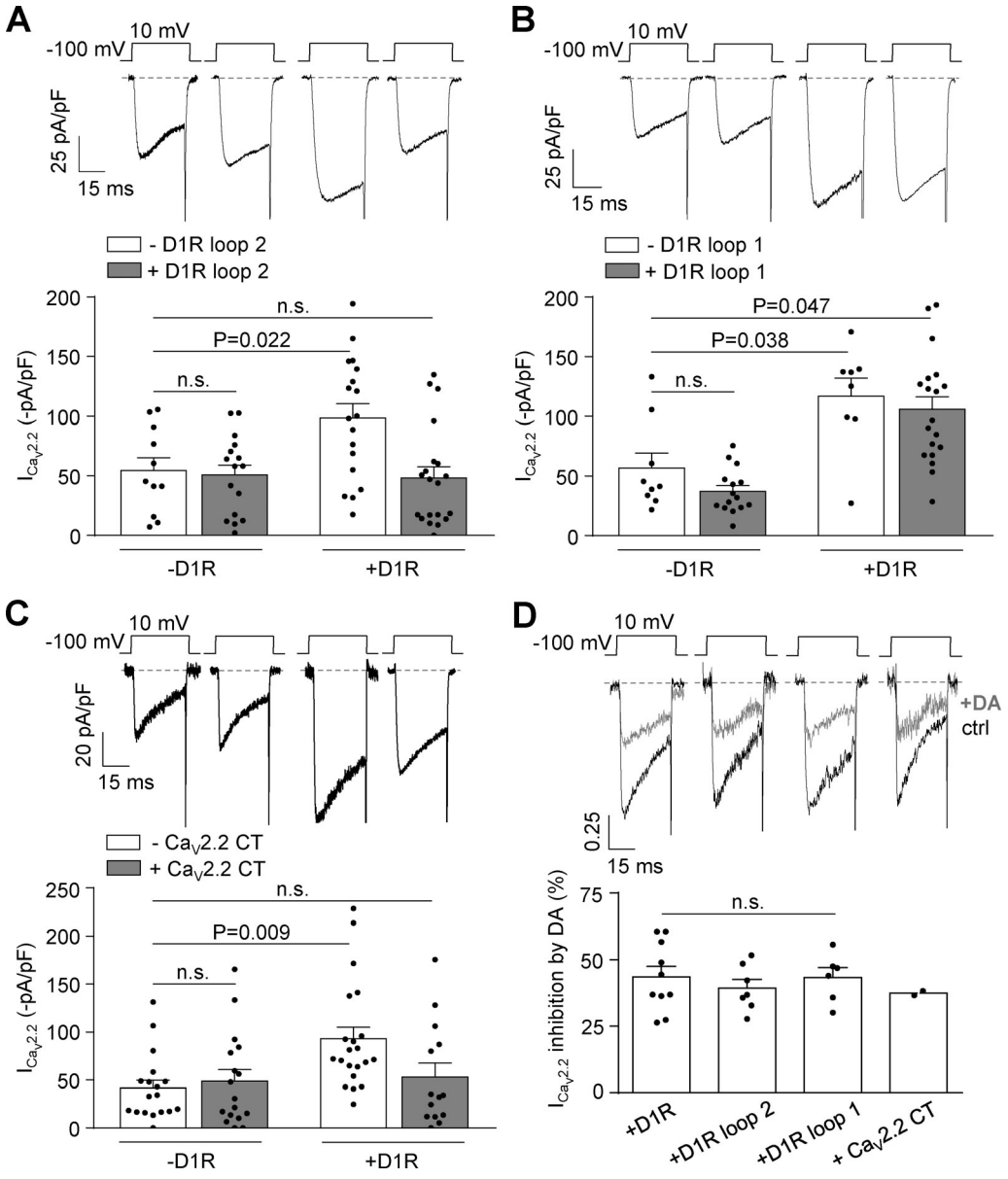

Figure 6. **$Ca_V2.2$ current increases caused by D1R constitutive activity are prevented by coexpression of D1R loop 2 and $Ca_V2.2$ C terminus without changes in dopamine-mediated $Ca_V2.2$ current inhibition in transfected HEK293T cells. (A)** Representative traces and averaged $Ca_V2.2$ currents ($I_{Cav2.2}$) from HEK293T cells cotransfected with $Ca_V2.2$, $Ca_V\alpha_2\delta_1$, $Ca_V\beta_3$, and either D1R (+D1R white bar; n = 18) or empty plasmid (−D1R white bar; n = 11), with (+D1R gray bar; n = 20) or without (−D1R gray bar; n = 16) D1R loop 2 (0.2 µg cDNA per well). **(B)** Representative traces and averaged $I_{Cav2.2}$ from HEK293T cells cotransfected with $Ca_V2.2$, $Ca_V\alpha_2\delta_1$, $Ca_V\beta_3$, and either D1R (+D1R white bar; n = 8) or empty plasmid (−D1R white bar; n = 9), with (+D1R gray bar; n = 19) or without (−D1R gray bar; n = 15) D1R loop 1 (0.2 µg cDNA per well). **(C)** Representative traces and averaged $Ca_V2.2$ currents ($I_{Cav2.2}$) from HEK293T cells cotransfected with $Ca_V2.2$, $Ca_V\alpha_2\delta_1$, $Ca_V\beta_3$, and either D1R (+D1R white bar; n = 21) or empty plasmid (−D1R white bar; n = 18), with (+D1R gray bar; n = 14) or without (−D1R gray bar; n = 17) proximal portion of $Ca_V2.2$ C terminus containing plasmid ($Ca_V2.2$ CT; 0.2 µg cDNA per well). **(D)** Representative traces and averaged percentage of inhibition of $I_{Cav2.2}$ by dopamine (+DA; 10 µM) in HEK293T cells coexpressing $Ca_V2.2$, $Ca_V\alpha_2\delta_1$, $Ca_V\beta_3$, and D1R (+D1R; n = 10), D1R plus D1R loop 2 (+loop 2; n = 7), D1R plus D1R loop 1 (+loop 1; n = 6), and D1R plus $Ca_V2.2$ CT (+$Ca_V2.2$ CT; n = 2). One-way ANOVA with Dunn's post-test versus −D1R white bar (A and C) and versus +D1R (D); Kruskal-Wallis test with Dunn's post-test versus −D1R white bar (B). n.s., nonstatistically significant. Data were expressed as mean ± SEM, and dots represent individual data points.

Q_{ON} increase is not due to changes in the relative open probability, we plotted raw Q_{ON} values versus peak tail current for individual cells (Wei et al., 1994; Jones et al., 1999; Takahashi et al., 2004; Garza-Lopez et al., 2018) and found that the parameters from the lineal regression fits for control cells (−D1R) and cells coexpressing D1R (+D1R) are not different (Fig. 7 B). Taken together, our experiments allow us to propose that D1R-$Ca_V2.2$ interaction is required for the increase in $Ca_V2.2$ current that occurs when constitutively active D1R is coexpressed. Additional biochemical experiments are required to conclude that the current enhancement by D1R constitutive activity correlates with a greater number of functional $Ca_V2.2$ channels in the plasma membrane.

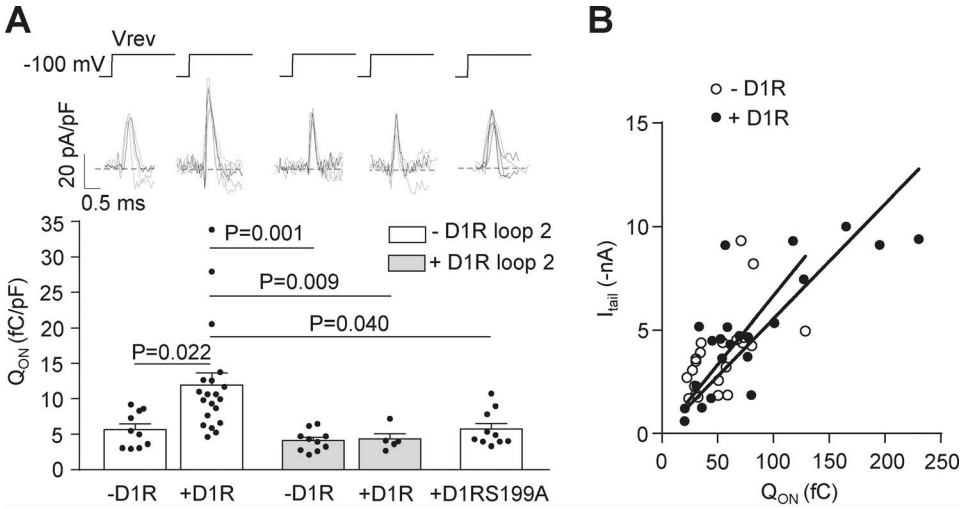

Figure 7. **D1R constitutive activity increases the number of functional $Ca_V2.2$ channels at the plasma membrane. (A)** Individual (gray) and averaged (black) traces of ON gating $Ca_V2.2$ currents (top panel) and averaged Q_{ON} from HEK293T cells cotransfected with $Ca_V2.2$, $Ca_V\alpha_2\delta_1$, $Ca_V\beta_3$, and either D1R (+D1R white bar; n = 17), D1RS199A (+D1RS199A white bar; n = 10), or empty plasmid (−D1R white bar; n = 10), with (+D1R gray bar; n = 5) or without (−D1R gray bar; n = 10) D1R loop 2 (0.2 µg cDNA per well; bottom panel). Reversal potential (V_{rev}, ∼60 mV) was estimated individually for each cell. **(B)** Q_{ON} versus peak $Ca_V2.2$ tail current (I_{tail} at −60 mV) plot for HEK293T cells coexpressing $Ca_V2.2$, $Ca_V\alpha_2\delta_1$, $Ca_V\beta_3$ with (+D1R black dots; n = 22, r^2 = 0.61) or without D1R (−D1R open dots; n = 22, r^2 = 0.31). Lineal regression slopes are not different between the groups (P = 0.187; F = 1.798). One-way ANOVA with Tukey's post-test (only significant comparisons shown, A). Extra sum of squares F test (B). pF, picofaradays. Data were expressed as mean ± SEM, and dots represent individual data points.

D1R constitutive activity effect on $Ca_V2.2$ requires Gs protein activity

We explored the requirement of Gs, the main G protein reported to couple to D1R, for the effect of D1R on $Ca_V2.2$ current. We first evaluated the changes in cAMP values driven by dopamine in our experimental system. We found that acute dopamine application increases cAMP levels, reaching a maximum value in 140 s in cells expressing D1R or D1R plus the loop 2 peptide. We also confirmed that chlorpromazine failed to increase cAMP in both experimental conditions as expected for the acute application of an inverse agonist (Fig. 8 A). We next quantified the basal cAMP by radioimmunoassay and found that it has a tendency to be larger in cells expressing D1R and is significantly larger in cells coexpressing D1R and loop 2 than in control cells (Fig. 8 B). These results suggest that Gs can be acutely activated on top of its basal level of activity and that the loop 2 does not alter Gs signaling. We next assayed the Gs inhibitor ChTx (500 ng/ml) in HEK293T cells. We first corroborated that ChTx occludes dopamine-induced inhibition of $Ca_V2.2$ currents in cells coexpressing D1R and the channel (Fig. 8 C). Finally, we assessed the effect of ChTx on basal currents and found that the toxin abolishes the increase in $Ca_V2.2$ currents induced by D1R coexpression (Fig. 8 D). Taken together, our results suggest that D1R constitutive activity signals through Gs, contributing to the increase in $Ca_V2.2$ currents (Fig. 8).

Our results indicate that D1R would interact with $Ca_V2.2$, increasing the amount of channels in plasma membrane depending on its constitutive activity. On the other hand, previous work that we have replicated here in part shows that dopamine-mediated D1R activity reduces $Ca_V2.2$ currents and promotes channel internalization (Huang and Zamponi, 2017). At this point, an open question is: why do D1R constitutive and dopamine-mediated activities have opposite effects? One possibility is that D1R places more channels in the membrane in order to amplify dopamine effects when it is released from near-synaptic terminals. If this were true, we would expect that in chlorpromazine-treated mice the capability of dopamine to inhibit $Ca_V2.2$ channels would be reduced, since there would be fewer channels available. In Fig. 9, we present data supporting this thought. We recorded native currents from mPFC neurons and reproduced the result from Fig. 1 showing that in chlorpromazine-treated animals, basal native Ca_V currents were reduced (Fig. 9 A). More importantly, the percentage of Ca_V current inhibition by 10 µM SKF38393 was significantly reduced in the chlorpromazine-treated group (Fig. 9 B).

Discussion

Here, we demonstrated that D1R constitutive activity increases $Ca_V2.2$ currents in a heterologous expression system. Based on our experiments using an inverse agonist and a D1R mutant lacking constitutive activity, we conclude that basally active D1Rs are required to increase $Ca_V2.2$ currents. Moreover, we confirmed that D1R loop 2 and the $Ca_V2.2$ C terminus occlude this effect, suggesting a direct interaction between D1R and the channel. Surprisingly, we found that Gs activity is also required, adding a new level of complexity to the mechanism. Taking into account a previous report by the Zamponi laboratory (Kisilevsky et al., 2008), we suggest that constitutively active D1R interacts with $Ca_V2.2$, stabilizing functional channels in the plasma membrane. In this context, active Gs protein could form part of the constitutively active D1R-$Ca_V2.2$ complex, or it could be exerting an additional effect by activating a cascade that somehow modifies the channel or D1R.

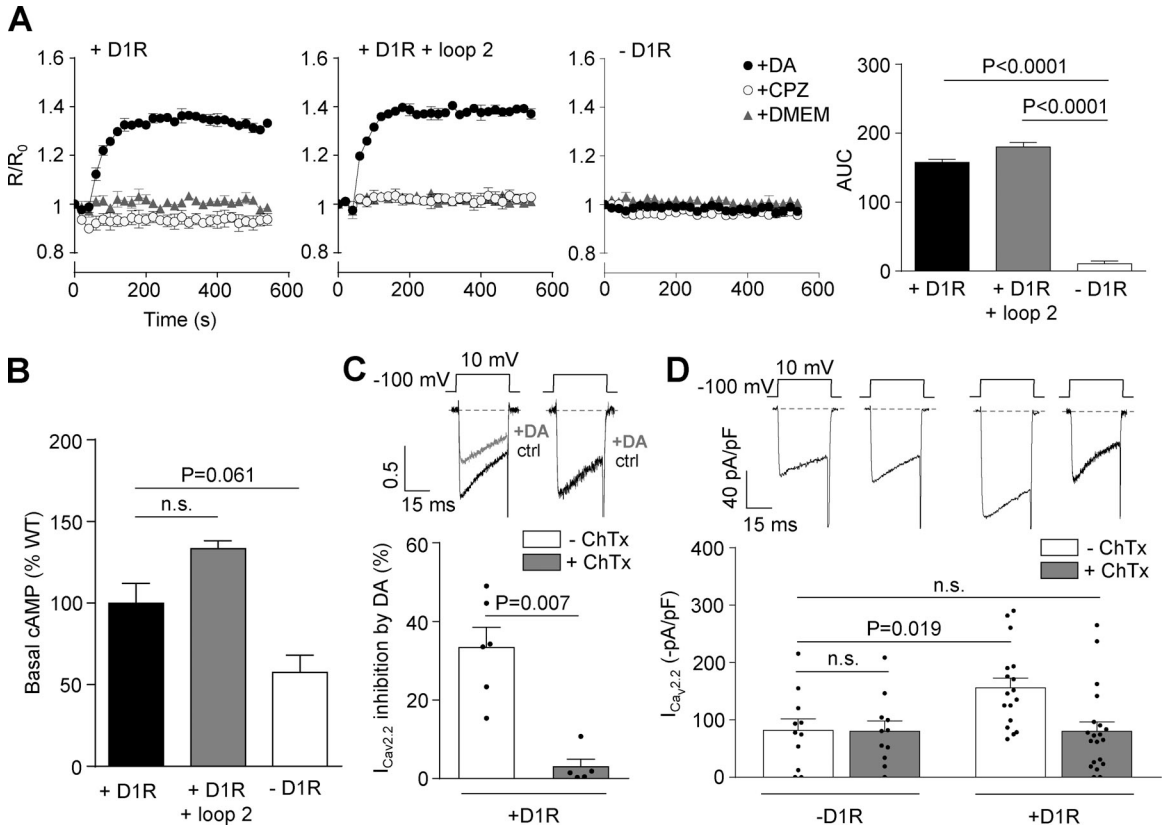

Figure 8. **D1R-induced increase in $Ca_V2.2$ currents requires Gs activation. (A)** Real-time cAMP time course recorded from HEK293T cells transfected with D1R (+D1R; $n = 3$), D1R plus D1R loop 2 (+D1R + loop 2; $n = 3$), and empty plasmid (−D1R; $n = 3$) with acute application of 1 µM dopamine (DA; black circles), 1 µM chlorpromazine (CPZ; white circles), and DMEM (gray triangles). Bars on the right represent R/Ro/540 s averaged values in the different conditions. **(B)** Basal measurement of cAMP values in HEK293T cells transfected with D1R (+D1R; $n = 6$), D1R plus D1R loop 2 (+D1R + loop 2; $n = 3$), and empty plasmid (−D1R; $n = 3$). **(C)** Representative traces and averaged percentage of inhibition of $Ca_V2.2$ currents ($I_{Cav2.2}$) by dopamine in HEK293T cells cotransfected with $Ca_V2.2$, $Ca_V\alpha_2\delta_1$, $Ca_V\beta_3$, and D1R preincubated or not with 500 ng/ml ChTx (+D1R −ChTx; $n = 6$) and (+D1R +ChTx; $n = 5$). **(D)** Representative traces and averaged $I_{Cav2.2}$ from HEK293T cells cotransfected with $Ca_V2.2$, $Ca_V\alpha_2\delta_1$, $Ca_V\beta_3$, and either D1R (+D1R −ChTx; $n = 17$) or empty plasmid (−D1R −ChTx; $n = 12$), preincubated or not with ChTx (−D1R +ChTx; $n = 11$) and (+D1R +ChTx; $n = 20$). One-way ANOVA with Dunn's post-test versus −D1R (A), versus +D1R (B), and versus −ChTx (C) and Student's unpaired t test (C). AUC, area under the curve; n.s., nonstatistically significant. Data were expressed as mean ± SEM, and dots represent individual data points.

Here, we propose that the chronic stimulatory effect of D1R coexpression requires Gs participation that would occur independently of Gs rapid activation by agonist binding to D1R. Our data demonstrate that basal levels of cAMP are elevated in cells expressing D1R and that acute dopamine application further increases these second messenger levels. Moreover, we found that ChTx, a specific Gs inhibitor, prevents $Ca_V2.2$ current increase by D1R coexpression as well as dopamine-induced acute $Ca_V2.2$ current inhibition. These opposite effects of D1R constitutive and dopamine-evoked activities on $Ca_V2.2$ current resemble other reports demonstrating that ORL-1 and D2R coexpression are capable of physically interacting and promoting channel traffic toward the plasma membrane, while the agonist-mediated activation of these GPCRs acutely reduces $Ca_V2.2$ current (Huang and Zamponi, 2017). Although it is not explored in these reports, GPCRs' constitutive activity could play a role in the basal increase of $Ca_V2.2$ trafficking. Indeed, there is evidence showing that ORL-1 (Beedle et al., 2004) and D2R (Akam and Strange, 2004; Roberts and Strange, 2005) display basal signaling. In the case of D2R, the constitutive activity is hard to evidence because D2R is coupled to Gi/o, and thus it reduces cAMP levels. On the other hand, a recent publication from our group suggests that D2R basal signaling through Gβγ impacts $Ca_V2.2$ currents (Cordisco Gonzalez et al., 2020). Thus, the dual opposite chronic and acute effects of D1R on $Ca_V2.2$ may be an example of a common modulatory behavior of some GPCRs.

We previously studied the effect of other basally active GPCRs on Ca_V currents with contrasting results. Ghrelin receptor constitutive activity reduces $Ca_V2.2$ forward trafficking from endoplasmic reticulum to plasma membrane and thus diminishes the $Ca_V2.2$ current in a Gi/o-dependent manner (Mustafá et al., 2017). On the other hand, melanocortin type 4 receptor reduces $Ca_V1.2$, $Ca_V1.3$, and $Ca_V2.1$ currents without affecting $Ca_V2.2$. Interestingly, melanocortin type 4 receptor is a Gs protein–coupled receptor, but its constitutive pathway acting on Ca_V currents is mediated by Gi/o (Agosti et al., 2014, 2017). This discrepancy reveals high heterogeneity among the effects of GPCR constitutive activity on Ca_V.

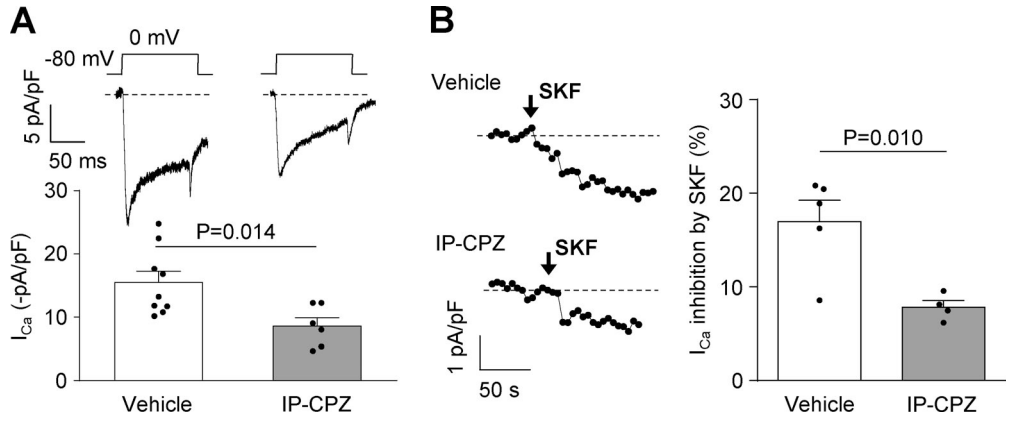

Figure 9. **Sensitivity of Ca_V currents from mPFC neurons to D1/D5R agonist is reduced in chlorpromazine IP–treated mice. (A)** Representative traces and averaged normalized Ca_V currents (I_{Ca}) registered in mPFC from mice treated IP with vehicle (n = 9, four animals) or chlorpromazine (CPZ; 1 mg/kg; n = 6, three animals). **(B)** Representative time courses of I_{Ca} and averaged percentage of I_{Ca} inhibition by SKF38393 (+SKF; 10 µM) in mPFC neurons from mice IP treated with vehicle (n = 5, four animals) or chlorpromazine (CPZ; 1 mg/kg; n = 4, three animals). Student's unpaired t test. Data were expressed as mean ± SEM, and dots represent individual data points.

Here, we found that injecting mice with IP chlorpromazine, an inverse agonist of D1/D5R, dramatically reduces calcium currents in mPFC neurons. By calculating the percentage of ω-conotoxin GVIA–sensitive current relative to the total current affected by chlorpromazine, we concluded that $Ca_V2.2$ accounts for ∼37% of the total calcium current reduced; thus, chlorpromazine also partially decreases non–ω-conotoxin GVIA–sensitive currents. One plausible explanation is that chlorpromazine acts directly on non-$Ca_V2.2$ subtypes of Ca_V. In this regard, an early work demonstrated that chlorpromazine acutely reduces L-type calcium current in cultured mouse neuroblastoma cells (Ogata et al., 1990). On the other hand, non-$Ca_V2.2$ subtypes could also be sensitive to D1/D5R constitutive activity. Further experiments are required to discriminate among the possibilities of a direct effect of chlorpromazine on non-$Ca_V2.2$ subtypes, a contribution of D5R constitutive activity to the total effect of chlorpromazine, and the targeting of non-$Ca_V2.2$ subtypes by D1R constitutive activity.

The effect of D1R on $Ca_V2.2$ occurs quite rapidly in mouse mPFC neurons. Less than 24 h are required to observe a current reduction by chlorpromazine injection, a time range comparable to the tens of hours reported for $Ca_V2.2$ turnover (Bernstein and Jones, 2007; Simms and Zamponi, 2012). Moreover, it has been described that the binding of dopamine induces both D1R and $Ca_V2.2$ internalization (Kisilevsky et al., 2008), and another study has shown that injection of methamphetamine, an inhibitor of dopamine reuptake, reduces Ca_V currents in a D1/D5R–dependent manner (González et al., 2016). Thus, it is possible that constitutively active D1R interacts with $Ca_V2.2$, preventing internalization and stabilizing the channel in the plasma membrane, and that dopamine binding to D1R reverts this effect. D1R-expressing neurons would thus display a highly dynamic regulation of $Ca_V2.2$ expression at the cell surface.

One putative function of D1R constitutive activity is to help specify $Ca_V2.2$ sub-cellular localization. D1R might play a role in the noncanonical somatic and dendritic sub-localization of $Ca_V2.2$. The receptor might also be part of a group of modulators that localize $Ca_V2.2$ to postsynaptic sites, particularly in layer V/VI pyramidal neurons of the mPFC. It was recently shown that the collapsing response mediator protein 2 (CRMP2) augments $Ca_V2.2$ protein in PFC neurons, an effect tied to cue reinstatement after cocaine self-administration extinction (Buchta et al., 2020). Thus, it is possible that $Ca_V2.2$, a typically presynaptic calcium channel, is playing a noncanonical role at postsynaptic sites in PFC neurons, and that D1R, among other modulators, stabilizes $Ca_V2.2$ protein at these sites. Here, we showed that Ca_V currents from animals IP injected with the D1R inverse agonist chlorpromazine are less sensitive to SKF-mediated inhibition. Considering that $Ca_V2.2$ is highly sensitive to G protein–signaling cascades, we postulate that neurons expressing constitutively active D1R would have larger calcium currents responsive to dopamine at postsynaptic sites. Moreover, it has been reported that $Ca_V2.2$ localizes in dendrites in cortical pyramidal and Purkinje cerebellar neurons (Westenbroek et al., 1992) and contributes to postsynaptic calcium entry in lumbar spinal cord neurons (Heinke et al., 2004) and dentate granule cells (Hamilton et al., 2010). It would be interesting to explore the role of high-density $Ca_V2.2$ at PFC postsynaptic sites in terms of its contribution to activity-mediated postsynaptic calcium entry, dendrite calcium potentials, and long-term plasticity.

Antipsychotic drugs are a large heterogeneous group of D1/D5R inverse agonists that were initially described as D2R antagonists (Cai et al., 1999; Martin et al., 2001). Our work proposes that basally active D1R can be a functional target of these drugs. Here, we used chlorpromazine, a typical antipsychotic drug, and found that D1R constitutive activity plays a role in controlling $Ca_V2.2$ current density. To our knowledge, this is the first clear functional output of D1R constitutive activity. Besides $Ca_V2.2$, other synaptic proteins may also be affected by D1R constitutive activity. In particular, in hippocampal neurons, NMDA receptors complex with D1R at perisynaptic sites, and dopamine binding unleashes NMDA receptors, which migrate to the synaptic sites and contribute to long-term potentiation (Ladepeche et al., 2013). It would be interesting to study the role of D1R constitutive activity in this mechanism. Meanwhile, D5R,

the other D1-like receptor, also displays basal activity. In this regard, the inhibition of D5R constitutive activity by flupenthixol, an atypical antipsychotic drug, depresses supranormal burst firing in subthalamic neurons in a rat model of Parkinson's disease (Chetrit et al., 2013). Thus, the study of the cellular and physiological effects of D1R-like receptor constitutive activity may help to improve treatments that rely on available antipsychotics, as well as to develop more efficient drugs.

Acknowledgments

Richard W. Aldrich served as guest editor.

We would like to thank Dr. Mario Tiberi for kindly donating the human D1R–containing plasmid; Dr. Diane Lipscombe (Brown University, Providence, RI) for providing the $Ca_V2.2$ subunits containing plasmids; Dr. Gerard Zamponi for kindly providing D1R loop 1– and loop 2–containing plasmids; Dr. KeesJalink for providing the mTurquoise2-EPAC-cp173Venus-Venus construct; and Dr. Mario Perello, Dr. Emilio R. Mustafá, and Priscilla McCarthy for carefully reading the manuscript.

This work was supported by grants from the National Agency of Scientific and Technological Promotion of Argentina (PICT2015-3330 and PICT 2017-0602 to J. Raingo and PICT 2017-2491 to A. Yaneff) and from the National University of La Plata (X768) to J. Raingo. C.I. McCarthy was supported by the National Agency of Scientific and Technological Promotion of Argentina; C. Chou-Freed was supported by the Fulbright U.S. Student Program; J. Raingo was supported by the National Scientific and Technical Research Council-Argentina; and S.S. Rodríguez was supported by the Scientific Research Committee of Buenos Aires (CIC), Argentina.

The authors declare no competing financial interests.

Author contributions: All experiments presented in this work were performed in the Electrophysiology Laboratory of IMBICE. J. Raingo directed the conception and experimental design, contributed to data interpretation, and was responsible for funding acquisition. S.S. Rodriguez planned and performed the directed mutation strategy for D1RS199A, obtained the cDNA constructs for D1R-YFP, D1RS199A-YFP, and $Ca_V2.2$ C terminus, and amplified and purified the clones for the HEK293T cells transient transfections. C. Chou-Freed cloned and amplified the D1R loop 1 and D1R loop 2 clones and participated in data acquisition and analysis. C.I. McCarthy performed data acquisition, analysis, and interpretation. J. Raingo and C.I. McCarthy prepared, wrote, and revised the manuscript. A. Yaneff performed the cAMP measurement, and C. Davio guided and designed these experiments. All authors have read, critically revised, and approved the final version of this manuscript and agree to be accountable for all aspects of the work in ensuring that questions related to the accuracy or integrity of any part of the work are appropriately investigated and resolved.

Submitted: 17 September 2019
Revised: 14 February 2020
Accepted: 12 March 2020

References

Agosti, F., E.J. López Soto, A. Cabral, D. Castrogiovanni, H.B. Schioth, M. Perelló, and J. Raingo. 2014. Melanocortin 4 receptor activation inhibits presynaptic N-type calcium channels in amygdaloid complex neurons. *Eur. J. Neurosci.* 40:2755–2765. https://doi.org/10.1111/ejn.12650

Agosti, F., S. Cordisco Gonzalez, V. Martinez Damonte, M.J. Tolosa, N. Di Siervi, H.B. Schioth, C. Davio, M. Perello, and J. Raingo. 2017. Melanocortin 4 receptor constitutive activity inhibits L-type voltage-gated calcium channels in neurons. *Neuroscience.* 346:102–112. https://doi.org/10.1016/j.neuroscience.2017.01.007

Akam, E., and P.G. Strange. 2004. Inverse agonist properties of atypical antipsychotic drugs. *Biochem. Pharmacol.* 67:2039–2045. https://doi.org/10.1016/j.bcp.2004.02.017

Al-Fulaij, M.A., Y. Ren, M. Beinborn, and A.S. Kopin. 2008. Pharmacological analysis of human D1 AND D2 dopamine receptor missense variants. *J. Mol. Neurosci.* 34:211. https://doi.org/10.1007/s12031-007-9030-x

Arnsten, A.F., M. Wang, and C.D. Paspalas. 2015. Dopamine's actions in primate prefrontal cortex: challenges for treating cognitive disorders. *Pharmacol. Rev.* 67:681–696. https://doi.org/10.1124/pr.115.010512

Beedle, A.M., J.E. McRory, O. Poirot, C.J. Doering, C. Altier, C. Barrere, J. Hamid, J. Nargeot, E. Bourinet, and G.W. Zamponi. 2004. Agonist-independent modulation of N-type calcium channels by ORL1 receptors. *Nat. Neurosci.* 7:118–125. https://doi.org/10.1038/nn1180

Bernstein, G.M., and O.T. Jones. 2007. Kinetics of internalization and degradation of N-type voltage-gated calcium channels: role of the α2/δ subunit. *Cell Calcium.* 41:27–40. https://doi.org/10.1016/j.ceca.2006.04.010

Buchta, W.C., A. Moutal, B. Hines, C. Garcia-Keller, A.C.W. Smith, P. Kalivas, R. Khanna, and A. Riegel. 2020. Dynamic CRMP2 regulation of CaV2.2 in the prefrontal cortex contributes to the reinstatement of cocaine seeking. *Mol. Neurobiol.* 57:346–357.

Cai, G., H. Gurdal, C. Smith, H.-Y. Wang, and E. Friedman. 1999. Inverse agonist properties of dopaminergic antagonists at the D(1A) dopamine receptor: uncoupling of the D(1A) dopamine receptor from G(s) protein. *Mol. Pharmacol.* 56:989–996. https://doi.org/10.1124/mol.56.5.989

Carozzo, A., A. Yaneff, N. Gómez, N. Di Siervi, A. Sahores, F. Diez, A.I. Attorresi, Á. Rodríguez-González, F. Monczor, N. Fernández, et al. 2019. Identification of MRP4/ABCC4 as a Target for Reducing the Proliferation of Pancreatic Ductal Adenocarcinoma Cells by Modulating the cAMP Efflux. *Mol. Pharmacol.* 96:13–25. https://doi.org/10.1124/mol.118.115444

Castiglioni, A.J., J. Raingo, and D. Lipscombe. 2006. Alternative splicing in the C-terminus of CaV2.2 controls expression and gating of N-type calcium channels. *J. Physiol.* 576:119–134. https://doi.org/10.1113/jphysiol.2006.115030

Chetrit, J., A. Taupignon, L. Froux, S. Morin, R. Bouali-Benazzouz, F. Naudet, N. Kadiri, C.E. Gross, B. Bioulac, and A. Benazzouz. 2013. Inhibiting subthalamic D5 receptor constitutive activity alleviates abnormal electrical activity and reverses motor impairment in a rat model of Parkinson's disease. *J. Neurosci.* 33:14840–14849. https://doi.org/10.1523/JNEUROSCI.0453-13.2013

Cools, R. 2008. Role of dopamine in the motivational and cognitive control of behavior. *Neuroscientist.* 14:381–395. https://doi.org/10.1177/1073858408317009

Cordisco Gonzalez, S., E.R. Mustafá, S.S. Rodriguez, M. Perello, and J. Raingo. 2020. Dopamine Receptor Type 2 and Ghrelin Receptor Coexpression Alters $Ca_V2.2$ Modulation by G Protein Signaling Cascades. *ACS Chem. Neurosci.* 11:3–13. https://doi.org/10.1021/acschemneuro.9b00426

Costa, T., and S. Cotecchia. 2005. Historical review: Negative efficacy and the constitutive activity of G-protein-coupled receptors. *Trends Pharmacol. Sci.* 26:618–624. https://doi.org/10.1016/j.tips.2005.10.009

Davio, C.A., G.P. Cricco, R.M. Bergoc, and E.S. Rivera. 1995. H1 and H2 histamine receptors in N-nitroso-N-methylurea (NMU)-induced carcinomas with atypical coupling to signal transducers. *Biochem. Pharmacol.* 50:91–96. https://doi.org/10.1016/0006-2952(95)00108-C

Garza-Lopez, E., J.A. Lopez, J. Hagen, R. Sheffer, V. Meiner, and A. Lee. 2018. Role of a conserved glutamine in the function of voltage-gated Ca^{2+} channels revealed by a mutation in human *CACNA1D*. *J. Biol. Chem.* 293:14444–14454. https://doi.org/10.1074/jbc.RA118.003681

Goldman-Rakic, P.S., S.A. Castner, T.H. Svensson, L.J. Siever, and G.V. Williams. 2004. Targeting the dopamine D1 receptor in schizophrenia: insights for cognitive dysfunction. *Psychopharmacology (Berl.).* 174:3–16. https://doi.org/10.1007/s00213-004-1793-y

González, B., C. Rivero-Echeto, J.A. Muñiz, J.L. Cadet, E. García-Rill, F.J. Urbano, and V. Bisagno. 2016. Methamphetamine blunts Ca(2+) currents

and excitatory synaptic transmission through D1/5 receptor-mediated mechanisms in the mouse medial prefrontal cortex. *Addict. Biol.* 21: 589–602. https://doi.org/10.1111/adb.12249

Hamilton, T.J., B.M. Wheatley, D.B. Sinclair, M. Bachmann, M.E. Larkum, and W.F. Colmers. 2010. Dopamine modulates synaptic plasticity in dendrites of rat and human dentate granule cells. *Proc. Natl. Acad. Sci. USA.* 107:18185–18190. https://doi.org/10.1073/pnas.1011558107

Heinke, B., E. Balzer, and J. Sandkühler. 2004. Pre- and postsynaptic contributions of voltage-dependent Ca2+ channels to nociceptive transmission in rat spinal lamina I neurons. *Eur. J. Neurosci.* 19:103–111. https://doi.org/10.1046/j.1460-9568.2003.03083.x

Herold, C., I. Joshi, O. Chehadi, M. Hollmann, and O. Güntürkün. 2012. Plasticity in D1-like receptor expression is associated with different components of cognitive processes. *PLoS One.* 7:e36484. https://doi.org/10.1371/journal.pone.0036484

Homberg, J.R., J.D. Olivier, M. VandenBroeke, J. Youn, A.K. Ellenbroek, P. Karel, L. Shan, R. van Boxtel, S. Ooms, M. Balemans, et al. 2016. The role of the dopamine D1 receptor in social cognition: studies using a novel genetic rat model. *Dis. Model. Mech.* 9:1147–1158. https://doi.org/10.1242/dmm.024752

Huang, J., and G.W. Zamponi. 2017. Regulation of voltage gated calcium channels by GPCRs and post-translational modification. *Curr. Opin. Pharmacol.* 32:1–8. https://doi.org/10.1016/j.coph.2016.10.001

Jones, M.W. 2002. A comparative review of rodent prefrontal cortex and working memory. *Curr. Mol. Med.* 2:639–647. https://doi.org/10.2174/1566524023361989

Jones, L.P., C.D. DeMaria, and D.T. Yue. 1999. N-type calcium channel inactivation probed by gating-current analysis. *Biophys. J.* 76:2530–2552. https://doi.org/10.1016/S0006-3495(99)77407-2

Kisilevsky, A.E., S.J. Mulligan, C. Altier, M.C. Iftinca, D. Varela, C. Tai, L. Chen, S. Hameed, J. Hamid, B.A. Macvicar, et al. 2008. D1 receptors physically interact with N-type calcium channels to regulate channel distribution and dendritic calcium entry. *Neuron.* 58:557–570. https://doi.org/10.1016/j.neuron.2008.03.002

Klarenbeek, J.B., J. Goedhart, M.A. Hink, T.W. Gadella, and K. Jalink. 2011. A mTurquoise-based cAMP sensor for both FLIM and ratiometric readout has improved dynamic range. *PLoS One.* 6:e19170. https://doi.org/10.1371/journal.pone.0019170

Kolata, S., K. Light, C.D. Wass, D. Colas-Zelin, D. Roy, and L.D. Matzel. 2010. A dopaminergic gene cluster in the prefrontal cortex predicts performance indicative of general intelligence in genetically heterogeneous mice. *PLoS One.* 5:e14036. https://doi.org/10.1371/journal.pone.0014036

Ladepeche, L., J.P. Dupuis, D. Bouchet, E. Doudnikoff, L. Yang, Y. Campagne, E. Bézard, E. Hosy, and L. Groc. 2013. Single-molecule imaging of the functional crosstalk between surface NMDA and dopamine D1 receptors. *Proc. Natl. Acad. Sci. USA.* 110:18005–18010. https://doi.org/10.1073/pnas.1310145110

López Soto, E.J., F. Agosti, A. Cabral, E.R. Mustafa, V.M. Damonte, M.A. Gandini, S. Rodríguez, D. Castrogiovanni, R. Felix, M. Perelló, et al. 2015. Constitutive and ghrelin-dependent GHSR1a activation impairs CaV2.1 and CaV2.2 currents in hypothalamic neurons. *J. Gen. Physiol.* 146:205–219. https://doi.org/10.1085/jgp.201511383

Martin, M.W., A.W. Scott, D.E. Johnston Jr., S. Griffin, and R.R. Luedtke. 2001. Typical antipsychotics exhibit inverse agonist activity at rat dopamine D1-like receptors expressed in Sf9 cells. *Eur. J. Pharmacol.* 420:73–82. https://doi.org/10.1016/S0014-2999(01)00982-7

Martínez Damonte, V., S.S. Rodríguez, and J. Raingo. 2018. Growth hormone secretagogue receptor constitutive activity impairs voltage-gated calcium channel-dependent inhibitory neurotransmission in hippocampal neurons. *J. Physiol.* 596:5415–5428. https://doi.org/10.1113/JP276256

McNab, F., A. Varrone, L. Farde, A. Jucaite, P. Bystritsky, H. Forssberg, and T. Klingberg. 2009. Changes in cortical dopamine D1 receptor binding associated with cognitive training. *Science.* 323:800–802. https://doi.org/10.1126/science.1166102

Meye, F.J., G.M. Ramakers, and R.A. Adan. 2014. The vital role of constitutive GPCR activity in the mesolimbic dopamine system. *Transl. Psychiatry.* 4: e361. https://doi.org/10.1038/tp.2013.130

Mustafá, E.R., E.J. López Soto, V. Martínez Damonte, S.S. Rodríguez, D. Lipscombe, and J. Raingo. 2017. Constitutive activity of the Ghrelin receptor reduces surface expression of voltage-gated Ca^{2+} channels in a $Ca_V\beta$-dependent manner. *J. Cell Sci.* 130:3907–3917. https://doi.org/10.1242/jcs.207886

Ogata, N., M. Yoshii, and T. Narahashi. 1990. Differential block of sodium and calcium channels by chlorpromazine in mouse neuroblastoma cells. *J. Physiol.* 420:165–183. https://doi.org/10.1113/jphysiol.1990.sp017906

Plouffe, B., J.-P. D'Aoust, V. Laquerre, B. Liang, and M. Tiberi. 2010. Probing the constitutive activity among dopamine D1 and D5 receptors and their mutants. Methods in Enzymology. Vol. 484. Academic Press, San Diego. 295–328.

Roberts, D.J., and P.G. Strange. 2005. Mechanisms of inverse agonist action at D2 dopamine receptors. *Br. J. Pharmacol.* 145:34–42. https://doi.org/10.1038/sj.bjp.0706073

Sawaguchi, T., and P.S. Goldman-Rakic. 1991. D1 dopamine receptors in prefrontal cortex: involvement in working memory. *Science.* 251: 947–950. https://doi.org/10.1126/science.1825731

Simms, B.A., and G.W. Zamponi. 2012. Trafficking and stability of voltage-gated calcium channels. *Cell. Mol. Life Sci.* 69:843–856. https://doi.org/10.1007/s00018-011-0843-y

Stubbendorff, C., E. Hale, H.J. Cassaday, T. Bast, and C.W. Stevenson. 2019. Dopamine D1-like receptors in the dorsomedial prefrontal cortex regulate contextual fear conditioning. *Psychopharmacology (Berl.).* 236: 1771–1782. https://doi.org/10.1007/s00213-018-5162-7

Svensson, K.A., B.A. Heinz, J.M. Schaus, J.P. Beck, J. Hao, J.H. Krushinski, M.R. Reinhard, M.P. Cohen, S.L. Hellman, B.G. Getman, et al. 2017. An Allosteric Potentiator of the Dopamine D1 Receptor Increases Locomotor Activity in Human D1 Knock-In Mice without Causing Stereotypy or Tachyphylaxis. *J. Pharmacol. Exp. Ther.* 360:117–128. https://doi.org/10.1124/jpet.116.236372

Takahashi, E., M. Ino, and T. Nagasu. 2004. Effect of genetic background on Cav2 channel alpha1 and beta subunit messenger RNA expression in cerebellum of N-type Ca2+ channel alpha1B subunit-deficient mice. *Comp. Med.* 54:690–694.

Thompson, J.L., D.R. Rosell, M. Slifstein, R.R. Girgis, X. Xu, Y. Ehrlich, L.S. Kegeles, E.A. Hazlett, A. Abi-Dargham, and L.J. Siever. 2014. Prefrontal dopamine D1 receptors and working memory in schizotypal personality disorder: a PET study with [^{11}C]NNC112. *Psychopharmacology (Berl.).* 231:4231–4240. https://doi.org/10.1007/s00213-014-3566-6

Wang, Y., G.L. Chan, J.E. Holden, T. Dobko, E. Mak, M. Schulzer, J.M. Huser, B.J. Snow, T.J. Ruth, D.B. Calne, et al. 1998. Age-dependent decline of dopamine D1 receptors in human brain: a PET study. *Synapse.* 30:56–61. https://doi.org/10.1002/(SICI)1098-2396(199809)30:1<56::AID-SYN7>3.0.CO;2-J

Wang, Y., H. Markram, P.H. Goodman, T.K. Berger, J. Ma, and P.S. Goldman-Rakic. 2006. Heterogeneity in the pyramidal network of the medial prefrontal cortex. *Nat. Neurosci.* 9:534–542. https://doi.org/10.1038/nn1670

Wass, C., A. Pizzo, B. Sauce, Y. Kawasumi, T. Sturzoiu, F. Ree, T. Otto, and L.D. Matzel. 2013. Dopamine D1 sensitivity in the prefrontal cortex predicts general cognitive abilities and is modulated by working memory training. *Learn. Mem.* 20:617–627. https://doi.org/10.1101/lm.031971.113

Wass, C., B. Sauce, A. Pizzo, and L.D. Matzel. 2018. Dopamine D1 receptor density in the mPFC responds to cognitive demands and receptor turnover contributes to general cognitive ability in mice. *Sci. Rep.* 8:4533. https://doi.org/10.1038/s41598-018-22668-0

Wei, X., A. Neely, A.E. Lacerda, R. Olcese, E. Stefani, E. Perez-Reyes, and L. Birnbaumer. 1994. Modification of Ca2+ channel activity by deletions at the carboxyl terminus of the cardiac alpha 1 subunit. *J. Biol. Chem.* 269: 1635–1640.

Westenbroek, R.E., J.W. Hell, C. Warner, S.J. Dubel, T.P. Snutch, and W.A. Catterall. 1992. Biochemical properties and subcellular distribution of an N-type calcium channel α 1 subunit. *Neuron.* 9:1099–1115. https://doi.org/10.1016/0896-6273(92)90069-P

Williams, G.V., and S.A. Castner. 2006. Under the curve: critical issues for elucidating D1 receptor function in working memory. *Neuroscience.* 139: 263–276. https://doi.org/10.1016/j.neuroscience.2005.09.028

Zahrt, J., J.R. Taylor, R.G. Mathew, and A.F. Arnsten. 1997. Supranormal stimulation of D1 dopamine receptors in the rodent prefrontal cortex impairs spatial working memory performance. *J. Neurosci.* 17: 8528–8535. https://doi.org/10.1523/JNEUROSCI.17-21-08528.1997

Zhang, B., A. Albaker, B. Plouffe, C. Lefebvre, and M. Tiberi. 2014. Constitutive activities and inverse agonism in dopamine receptors. Advances in Pharmacology. Vol. 70. Elsevier, New York. 175–214.

Zhang, B., X. Yang, and M. Tiberi. 2015. Functional importance of two conserved residues in intracellular loop 1 and transmembrane region 2 of Family A GPCRs: insights from ligand binding and signal transduction responses of D1 and D5 dopaminergic receptor mutants. *Cell. Signal.* 27: 2014–2025. https://doi.org/10.1016/j.cellsig.2015.07.006